Published in final edited form as:
Immunol Lett. 2005 June 15; 99(1): 36–44. doi:10.1016/j.imlet.2004.12.010.

Intestinal TSH production is localized in crypt enterocytes and in villus 'hotblocks' and is coupled to IL-7 production: evidence for involvement of TSH during acute enteric virus infection

Virginia L. Scofield[1], **Dina Montufar-Solis**[3], **Elly Cheng**[2], **Mary K. Estes**[2], and **John R. Klein**[3,*]

[1] Department of Carcinogenesis, The University of Texas M.D. Anderson Cancer Center, Science Park-Research Division, Smithville, TX, USA

[2] Department of Molecular Virology and Microbiology, Baylor College of Medicine, Houston, TX, USA

[3] Department of Diagnostic Sciences, Dental Branch, University of Texas Health Science Center at Houston, Houston, TX, USA

Abstract

The immune and neuroendocrine systems have been shown to work conjointly in a number of ways. One aspect of this has to do with a potential role for thyroid stimulating hormone (TSH) in the regulation of the mucosal immune system, although the mechanisms by which this occurs remain vague. To more thoroughly understand how TSH participates in intestinal intraepithelial lymphocyte (IEL) development and immunity, experiments have been conducted to define local sites of intestinal TSH production, and to characterize changes that occur in the synthesis of TSH during acute enteric virus infection. Here, we demonstrate that TSH in the small intestine is specifically localized to regions below villus crypts as seen by immunocytochemical staining, which revealed high-level TSH staining in lower crypts in the absence of IL-7 staining, and TSH and IL-7 costaining in upper crypt regions. Additionally, prominent TSH staining was evident in TSH 'hotblocks' sparsely dispersed throughout the epithelial layer. In rotavirus-infected mice, the TSH staining pattern differed significantly from that of non-infected animals. Notably, at 2 and 3 days post-infection, TSH expression was high in and near apical villi where virus infection was greatest. These findings lend credence to the notion that TSH plays a role both in the development of intestinal T cells, and in the process of local immunity during enteric virus infection.

Keywords

Enteric; hormone; endocrine; immunity; rotavirus

1. Introduction

T cells located in the intestinal epithelium, the intraepithelial lymphocytes (IELs), differ from those that have matured in the thymus in several important respects. First, an unusually high proportion of IELs in mice are γδ T cells, although αβ T cells are also well represented [1,2]. Second, unlike peripheral $CD8^+$ T cells, most IELs express a homodimeric CD8αα complex

Corresponding author: John R. Klein, University of Texas Health Science Center, Department of Diagnostic Sciences, Rm. 3.094F, Dental Branch, 6516 M.D. Anderson Blvd., Houston, TX 77030, TEL: 713-500-4369, FAX: 713-500-4416, john.r.klein@uth.tmc.edu.

[2]. Third, some IELs can recognize and respond to nonclassical major histocompatibility complex molecules [3,4] and heat shock proteins [5], which may be linked to CD8αα expression by IELs. Fourth, the mammalian intestine can promote the differentiation of T cell precursors from bone marrow progenitors [6–8], and the intestine appears to provide both contact-mediated and humoral components necessary for the maturation of T cells [9]. Consistent with that, developing IELs have receptors for IL-7 and use IL-7 for survival and maturation [10, 11].

Based on gene expression studies, previous work from our laboratory revealed that small intestinal epithelial cells express genes for thyrotropin-releasing hormone (TRH) and thyroid stimulating hormone (TSH), and that intestinal IELs express the TSH receptor (TSHR) gene [12]. Exogenous supplementation of mice with TRH or TSH expanded the TCRαβ but not the TCRγδ subset [13,14]. Moreover, mice with defective TSH receptor have reduced numbers of TCRαβ IELs [12]. Collectively, those findings point to a novel epithelial-lymphocyte hormone loop consisting of TSH production by epithelial cells and TSH utilization by IELs. Although the significance of that paracrine immune-endocrine network has not been fully determined, we speculated that it contributes to the development and/or differentiation of IELs, or that it may be involved in the activation of IELs in response to antigen [15].

In order to better define the functional role of TSH in the murine small intestine, we have conducted a series of experiments from two perspectives. First, *in situ* experiments have been done to localize areas within the intestinal mucosa where TSH synthesis occurs. Second, we have used an experimental system involving rotavirus — a natural infectious agent of mice — to compare the changes that occur in TSH production between normal non-infected mice and mice with acute virus infection. Here, we report several new features of the intestinal TSH immune-endocrine network in that: (i) TSH expression is characteristically found among differentiating IL-7^+ and c-kit^+ small intestinal cryptopatches; (ii) intestinal TSH production also occurs in discrete regions of mature enterocytes covering luminal villi; and (iii) TSH expression is upregulated in site-specific locations associated with rotavirus infection. These findings point to a dynamic and intimate relationship between TSH and intestinal IELs at sites believed to be areas of local IEL development, and they point to a close association between TSH expression and enteric virus infection at the level of the intestinal epithelium.

2. Materials and methods

2.1 Mice

C57BL/6J and BALB/c mice were purchased from The Jackson Laboratory (Bar Harbor, ME). BALB/c mice were purchased from Harlan Sprague-Dawley (Houston, TX). Mice were used in accordance with institutional animal welfare guidelines.

2.2 Antibodies and reagents

The anti-mouse TSH monoclonal antibody, 1B11, was produced [16] and biotinylated [17] in our laboratory. PE-anti-CD4 (GK1.5), FITC-anti-CD8 (53–6.7), biotinylated anti-c-kit (2B8), biotinylated mouse Ig (G155-228), purified anti-mouse CD16/CD32 (2.4G2) mAbs, streptavidin-FITC, and streptavidin-APC, and were purchased from BD-PharMingen (San Diego, CA). Goat anti-IL-7 antibody (AB-407-NA) was purchased from R&D Systems, Inc. (Minneapolis, MN). Texas Red-conjugated donkey anti-goat (cat. no. 705-076-147) and anti-rabbit (cat. no. 711-076-152) antibodies were purchased from Jackson Immunoresearch Laboratories (West Grove, PA). Anti-rotavirus antibodies were produced by immunization of rabbits with virus-like particles (VLPs) assembled *in vitro* from the VP2 and VP6 structural proteins of simian rotavirus SA11 clone 3 [19]. Bovine TSH (Sigma Chemicals, T8931; St. Louis, MO), used for studies of TSHR expression, was biotinylated [17] in our laboratory.

2.3 Virus infection

Six- to eight-week old BALB/c mice were infected orally with 100 ul of culture medium containing 10^4 SD_{50} of the EC-WT rotavirus [18]. Non-infected control mice were given PBS. At days 2 and 3 days after infection, duodenal tissues from infected and non-infected control mice were removed and processed for immunofluorescence analysis as described below.

2.4 Immunofluorescence staining

Five- to six-week-old BALB/c or C57BL/6 mice were euthanized with CO_2 inhalation and cervical dislocation. 2 cm sections of the small intestinal jejunum were removed, placed into Tissue-Tek OCT embedding medium (Electron Microscopy Sciences; Hatfield, PA), and snap-frozen in liquid N_2. Blocks were cut into 5 uM serial sections on a ThermoShandon Motorized Electronic Cryotome (Pittsburg, PA); 20–40 sections were cut per specimen from each mouse. Sections on slides were fixed in acetone for 5 minutes. Prior to staining, tissues were reacted for 15 minutes with biotin blocking solution, 15 minutes in avidin blocking solution (Vector Laboratories; Burlingame, CA). Individual sections were incubated overnight at 4°C with 10–20 ug/ml 1B11 and/or anti-IL-7 antibodies. After washing with PBS, the sections were incubated in the dark with streptavidin-FITC and/or Texas Red-conjugated donkey anti-goat Ig for 1 hour, washed with PBS, and mounted for observation. For detection of rotavirus infection, both anti-rotavirus antibodies were used together as primary antibodies at a 1:100 dilution, incubated overnight at 4°C. Sections were washed with PBS and reacted with Texas-Red-conjugated anti-rabbit IgG antibody at 10–30 ul/100 ml. Control slides were incubated with biotinylated mouse Ig antibodies followed by streptavidin-FITC (for nonspecific binding by 1B11) or with affinity-purified goat IgG followed by Texas Red-conjugated donkey anti-goat antibody. Immunofluorescence analyses were done with an Olympus ProVis AX70 microscope or an Olympus Bh-2 fluorescence microscope (Olympus America; Melville, NY). Images were analyzed using Image-Pro Plus software (Media Cybernetics; Silver Spring, MD).

2.5 TSHR staining

For TSHR staining, small intestinal IELs were recovered as previously described [20] and suspended in 100 ul of TSH staining buffer (PBS containing 0.2 M sucrose, 0.1% NaN_3 0.1% BSA pH 7.4) [21,22]. The cells were incubated for 10 min with 2 ul of purified anti-CD16/CD32 mAb; this was done to prevent non-specific binding of anti-CD4 and anti-CD8 antibodies via Fc receptors. Cells were incubated for 30 min at 4°C with 4 ug of biotinylated bovine TSH and 1 ug/ml of PE-anti-CD4 and FITC-anti-CD8α mAbs. Cells were washed and reacted for 20 min at 4°C with streptavidin-APC, washed, fixed in 2% formalin. Cells were analyzed using a FACScalibur flow cytometer (Becton Dickinson; San Jose, CA); data were analyzed using CELLquest software (Beckton Dickinson). Specific TSH binding was determined based on reactivity of cells to streptavidin-APC in the absence of biotinylated TSH.

3. Results

3.1 TSH is expressed in normal crypt enterocytes and in villus enterocyte ‘hotblocks’

Frozen section tissues of normal small intestinal jejunum were incubated with biotinylated 1B11 (a mAb to mouse TSHβ) [16], or with biotinylated mouse Ig followed by streptavidin-FITC. All studies were done using jejunum tissues in order to standardize specimen analysis. No staining was observed throughout tissues using control mAb (Fig. 1A,B). In contrast, localized TSH staining was evident is crypt regions of the intestinal mucosa (Fig. 1C,D, yellow arrows). In tissue sections from six mice, 9.4 ± 2.6 TSH^+ crypt-staining areas were present per tissue at 100x magnification. A typical example of this is shown in Fig. 2B. TSH staining was also evident in the base of some villus crypts and in areas just proximal to those areas (Fig. 1C,D, red arrows). Although in some cases the intensity of staining in the latter areas was lower

than in crypt regions (Fig. 2B,C), specific staining was nonetheless evident above background levels (Fig. 2A). Finally, a second distinguishing feature of the TSH staining in jejunal tissues was the presence of focal 'hotblocks' of bright TSH staining in apical-lateral portions of some villi. A characteristic pattern of this is shown in Fig. 1E,F.

3.2 TSH staining is located in IL-7$^+$ cryptopatches

Cryptopatches are regions in the intestinal mucosa believed to be involved in intestinal T cell development and/or differentiation [6,11,23]. IL-7 and c-kit staining has been shown to be a characteristic feature of cryptopatches [6,11,23]. To determine whether TSH synthesis was linked to cryptopatch regions, two experiments were done. In the first, jejunal tissue sections were stained with anti-c-kit antibody as a means of locating cryptopatches in the mucosa. In the second, jejunal tissue sections were stained with both anti-TSH and anti-IL-7 antibodies as described in the Materials and methods to determine whether both were co-expressed by crypt epithelial cells. Fig. 2D shows that clusters of c-kit-stained cells were abundant above the muscularis mucosae in areas where TSH staining also was prominent (see Fig. 2B). Stronger evidence supporting an association of TSH synthesis and cryptopatches was evident from staining with both anti-TSH and anti-IL-7 antibodies. As shown in Fig. 3A, TSH staining was evident in two areas of crypt mucosa — one proximal to the muscularis and in the area slightly distal to that. IL-7 staining was located in the latter region (Fig. 3B). When these images were overlaid, clear evidence of TSH and IL-7 staining could be seen (Fig. 3C). Taken together, these findings make a strong case for TSH production in cryptopatch areas.

3.3 TSH staining is minimal in liver and kidney

The findings described above, particularly the extent to which TSH staining was localized in areas within the intestine, supported the idea that TSH is selectively produced in regions of the small intestine. To determine the extent to which TSH production might also occur in extra-intestinal tissues, liver and kidney tissue sections were stained with the anti-TSH mAb, 1B11, or with control antibodies using the same protocols and concentrations applied to intestinal tissues. As seen in Fig. 4, no significant difference was observed in the level of TSH staining in liver (Fig. 4C) compared to liver control staining (Fig. 4A). This also held true for staining of kidney sections when comparing TSH staining (Fig. 4D) to. kidney control staining (Fig. 4B).

3.4 The TSH receptor is expressed on all major IEL subsets defined by CD4 and/or CD8 expression, but is predominantly affiliated with CD8$^+$ cells

The fact that TSH expression was not uniformly expressed throughout the intestinal mucosa prompted us to determine which population(s) of IELs express the TSHR in order to predict which IELs are most responsive to TSH utilization. To assess the reactivity of IELs for TSHR expression by flow cytometry, biotinylated bovine TSH plus streptavidin-APC was used according to procedures previously described by our [21,26] and other [22] laboratories, in conjunction with staining for CD4 and CD8 expression. As shown in Fig. 5, the TSHR was expressed on a subpopulation of the total IELs, which in this experiment constituted 22.1% of the total cells. Of several mice studied (N = 8), 19.3 ± 3.4% of the IELs overall expressed the TSHR. Among the TSHR$^+$ IELs, ~three-fourths were CD8$^+$ cells, which included a subset CD4$^-$CD8$^+$ cells and a subset of CD4$^+$CD8$^+$ cells. The latter IEL population, which is reproducibly present in IEL isolates [24], may have immunoregulatory properties [25]. The remaining one-fourth of the TSHR$^+$ cells was either CD4$^+$CD8$^-$ cells or CD8$^-$CD4$^-$ cells. These findings indicate that TSH responsive cells are not universally represented among the IELs, and they suggest that TSH utilization is distributed across several distinct groups of intestinal T cells.

3.5 TSH expression in enterocytes of distal villi is upregulated during rotavirus infection

Rotaviruses are double-stranded RNA viruses that cause diarrheal diseases in birds and mammals. Infection is specific for distal villi in the small and large intestine [27]. To determine whether TSH expression was affected by virus infection, frozen sections of the jejunum from non-infected and infected mice, euthanized on day 2 and day 3 after infection, were stained with rabbit anti-rotavirus antiserum and biotinylated anti-TSH antibody followed by donkey Texas Red-conjugated anti-rabbit IgG and streptavidin-FITC. Fig. 6A shows that rabbit anti-rotavirus antibody was non-reactive with small intestine tissues from non-infected mice. TSH staining of that section revealed staining in crypt regions and hotblocks, with little if any staining along villus tips (Fig. 6B). In tissues from day 2 rotavirus-infected mice, anti-rotavirus staining was clearly evident in apical villus tips where virus infection is greatest (Fig. 6C,E,G; Fig. 7D). In addition, at day 2 of virus infection there was a high level of TSH staining that extended out into apical villi (Fig. 6D,F,H; Fig. 7C). Similar TSH (Fig. 7E,G) and anti-rotavirus (Fig. 7F,H) staining of villus tip enterocytes was evident in jejunum sections from animals at day 3 of infection. Intestinal tissues from rotavirus-infected mice did not stain with control FITC reagent (Fig. 7A), indicating that the increase in TSH staining observed in virus-infected tissues was not due to a non-specific effect of infection.

4. Discussion

The pattern of anti-TSH and anti-IL-7 antibody binding in normal mouse intestines (Fig. 1–3) shows that expression of both markers is a tightly localized activity of enterocytes in specific locations in the crypt-villus axis, rather than of all enterocytes in the small intestinal mucosae. Since enterocytes are “born” in the crypts from stem cells whose progeny move up the villi as the cells divide [6,23], the layered presence of TSH and IL-7 in the crypt area is consistent with a role for both proteins in early T cell development in this area of the small intestine. On the other hand, the localized expression of TSH by blocks of distal enterocytes near the tips of villi could reflect either *de novo* activation of TSH production in response to enterocyte or mucosal damage, or antigen contact by enteric antigen-presenting cells and dendritic cells [28,29]. Jejunal tissues were used in this study to standardize analysis. It is possible that differences in TSH expression exist in other areas of the small or large intestine. An extensive study of those tissues is planned.

Although we have not identified the factors responsible for TSH expression in hotblocks from intestines of normal healthy mice, it is significant that enterocytes containing rotavirus, and manifesting other signs of infection (cytoskeletal disorganization and shedding from the mucosal layer), are also positive for TSH. It is possible that enterocytes activated by nonviral influences in non-infected mice are differentially susceptible to rotavirus infection. However, the observations reported here suggest instead that the condition of infection itself is responsible for TSH expression in these distinct virus-infected regions. If this is so, then TSH may be re-activated in infected cells and in their neighbors, either as direct responses by the enterocytes to stress signals inside the cells, or as indirect responses to cytokines or other humoral factors produced by activated IELs or T cells in or underlying the infected mucosal cell layer. In either case, this observation couples TSH and IL-7 expression by enterocytes to enterocyte infection, and depicts a local microenvironment in which T cell survival and growth factors are made available in increased amounts in areas where augmentation of local defenses may be required.

In the adult mouse thymus, IL-7 is also expressed by epithelial cells in a layered pattern, with most immunoreactive IL-7 being present at the corticomedullary junction where $CD34^+$ bone marrow T cell precursors arrive in the thymus, and in the subcapsular region where T cell progenitors complete the $CD44^+25^-$ to $CD44^-CD25^+$ transition. It is tempting to speculate that intestinal T cells near the two layers of crypt enterocytes expressing TSH and/or IL-7 (Fig. 3)

are partitioned in a similar way, with newly arrived progenitors located in the cryptopatches and lower villus lamina propria that is overlaid by more mature lamina propria T cells and IELs distal portions of the villi. Mature intestinal T cells and IELs are partially activated [30], but they may be fully activated in areas where TSH is available.

These findings also have implications for understanding the ontogenic relationship between the immune and endocrine systems, particularly as they relate to the gastrointestinal tract. There now is evidence that T cells in conjunction with thyroid hormones from the thymus and the thyroid, which are pharyngeal endoderm derivatives [31–33], act together with intestinal T cells to control the cellularity, function and integrity of the chordate intestine, an organ formed from hindgut endoderm [34–35]. This functional interdependence may reflect an ancient relationship, characteristic of all vertebrates, between thyroid hormones and T cells regardless of their origin (thymus or intestine). In early invertebrate and vertebrate chordates, and in their modern descendants (tunicates, amphioxus and larval lampreys), the gut tube includes the pharynx, which acts as a filter-feeding organ, and the endostyle, a thyroid homologue [36]. In higher vertebrates, the pharynx is part of the upper respiratory tract, and the thyroid is an endocrine gland that is no longer connected to the pharynx or gut.

Tunicates, amphioxus, and lampreys are primitive chordates that lack a thymus and do not have adaptive immunity, but which do have an endostyle and thyroid hormones [37,38]. In lampreys, lymphocyte-like cells are located in the larval intestine, both in the connective tissue underlying the mucosa and in the mucosal cell layer itself [39,40]. These locations are analogous to those in which mammalian intestinal T cells are found. These parallels are consistent with the idea that the pharyngeal thymus and intestine of advanced vertebrates may be highly-differentiated remnants of what once was a continuous pharynx-intestine gut tube. In such a structure, it is likely that the epithelium interacted closely with lymphoid cells via thyroid hormones along the entire length of the tract. We suggest that vertebrate T cell differentiation and activation are controlled, at least in part, by thyroid axis hormones regardless of the location or origin of the T cells (thymus, lymph node, spleen, or intestine). The findings reported here, as well as those demonstrating a direct role for TSH in bone remodeling [41], add to the growing body of information indicating that TSH is a multidimensional molecule with properties that extend beyond the neuroendocrine system [42].

Acknowledgments

Supported by NIH Grants DK35566, DK30144, and DK56338.

References

1. Chen Y, Chou K, Fuchs E, Havran WL, Boismenu R. Protection of the intestinal mucosa by intraepithelial γδ T cells. Proc Natl Acad Sci (USA) 2002;99:14338–43. [PubMed: 12376619]
2. Guy-Grand D, Vassalli P. Gut intraepithelial lymphocyte development. Curr Opin Immunol 2002;14:255–59. [PubMed: 11869901]
3. Leishman AJ, Naidenko OV, Attinger A, Koning F, Lena CJ, Xiong Y, Chang HC, Reinherz E, Kronenberg M, Cheroutre H. T cell responses modulated through interaction between CD8αα and the nonclassical MHC Class I molecule, TL. Science 2001;294:1936–39. [PubMed: 11729321]
4. Das G, Gould DS, Augustine MM, Fragoso G, Sciutto E, Stroynowski I, Van Kaer L, Schust DJ, Ploegh H, Janeway CA Jr, Scitto E. Qa-2-dependent selection of CD8αα T cell receptorαβ$^+$ cells in murine intestinal intraepithelial lymphocytes. J Exp Med 2000;192:1521–28. [PubMed: 11085754]
5. Kim HT, Nelson EL, Clayberger C, Sanjanwala M, Sklar J, Krensky AM. γδ T cell recognition of tumor Ig peptide. J Immunol 1995;154:1614–23. [PubMed: 7836746]
6. Ishikawa H, Saito H, Suzuki K, Oida T, Kanamori Y. New gut-associated lymphoid tissue "cryptopatches" breed murine intestinal intraepithelial T cell precursors. Immunol Res 1999;20:253–60.

7. Oida T, Suzuki K, Nanno M, Kanamori Y, Saito H, Kubota E, Kato S, Itoh M, Kaminogawa S, Ishikawa H. Role of gut cryptopatches in early extrathymic maturation of intestinal intraepithelial T cells. J Immunol 2000;164:3616–26. [PubMed: 10725718]
8. Suzuki K, Oida T, Hamada H, Hitotsumatsu O, Watanabe M, Hibi T, Yamamoto H, Kubota E, Kaminogawa S, Ishikawa H. Gut cryptopatches: direct evidence of extrathymic anatomical sites for intestinal T lymphopoiesis. Immunity 2000;13:691–702. [PubMed: 11114381]
9. Lambolez F, Azogui O, Joret AM, Garcia C, von Boehmer H, Di Santo J, Ezine S, Rocha B. Characterization of T cell differentiation in the murine gut. J Exp Med 2002;195:437–39. [PubMed: 11854357]
10. Yada S, Nukina H, Kishihara K, Takamura N, Yoshida H, Inagaki-Ohara K, Nomoto K, Lin T. IL-7 prevents both caspase-dependent and – independent pathways that lead to the spontaneous apoptosis of i-IEL. Cell Immunol 2001;208:88–95. [PubMed: 11333141]
11. Laky K, Lefrancois L, Lingenheld GG, Ishikawa H, Lewis JM, Olson S, Suzuki K, Tigelaar RE, Puddington L. Enterocyte expression of interleukin-7 induces development of γδ T cells and Peyer's patches. J Exp Med 2000;191:1569–80. [PubMed: 10790431]
12. Wang J, Whetsell M, Klein JR. Local hormone networks and intestinal T cell homeostasis. Science 1997;275:1937–39. [PubMed: 9072972]
13. Wang J, Klein JR. Thymus-neuroendocrine interactions in extrathymic T cell development. Science 1994;265:1860–62. [PubMed: 8091211]
14. Wang J, Klein JR. Hormonal regulation of extrathymic gut T cell development: Involvement of thyroid stimulating hormone. Cell Immunol 1995;161:299–302. [PubMed: 7697742]
15. Klein J. T cell development within the intestinal mocosa: clues to a novel immune-endocrine network? Adv Neuroimmunol 1996;6:397–405. [PubMed: 9183519]
16. Zhou Q, Wang HC, Klein JR. Characterization of novel anti-mouse thyrotropin monoclonal antibodies. Hybrid Hybridomics 2002;21:75–79. [PubMed: 11991820]
17. Harlow, E.; Lane, L. Antibodies: A Laboratory Manual. Cold Spring Harbor, NY: Cold Spring Harbor Laboratory Press; 1988.
18. Crawford SE, Estes MK, Ciarlet M, Barone C, O'Neal CM, Cohen J, Conner ME. Heterotypic protection and induction of a broad heterotypic neutralization response by rotavirus-like particles. J Virol 1999;73:4813–22. [PubMed: 10233942]
19. Ciarlet M, Crawford SE, Barone C, Bertolotti-Ciarlet A, Ramig RF, Estes MK, Conner ME. Subunit rotavirus vaccine administered parenterally to rabbits induces active protective immunity. J Virol 1998;72:9233–46. [PubMed: 9765471]
20. Wang HC, Klein JR. Multiple levels of activation of murine $CD8^+$ intraepithelial lymphocytes defined by OX40 (CD134) expression: Effects on cell-mediated cytotoxicity, IFN-γ, and IL-10 regulation. J Immunol 2001;167:6717–23. [PubMed: 11739485]
21. Bagriacik EU, Klein JR. The thyrotropin (thyroid-stimulating hormone) receptor is expressed on murine dendritic cells and on a subset of $CD45RB^{high}$ lymph node T cells: functional role for thyroid-stimulating hormone in immune activation. J Immunol 2000;164:6158–65. [PubMed: 10843665]
22. Coutelier JP, Kehrl JH, Bellur SS, Kohn LD, Notkins AD, Prabhakar BS. Binding and functional effects of thyroid stimulating hormone on human immune cells. J Clin Immunol 1990;10:204–10. [PubMed: 2170438]
23. Kanamori Y, Ishimaru K, Nanno M, Maki K, Ikuta K, Nariuchi H, Ishikawa H. Identification of a novel lymphoid tissue in murine intestinal mucosa where clusters of $c\text{-}kit^+$ $IL\text{-}7R^+$ $Thy\text{-}1^+$ lympho-hematopoietic progenitors develop. J Exp Med 1996;184:1449–59. [PubMed: 8879216]
24. Mosley RL, Styre D, Klein JR. CD4+CD8+ murine intestinal intraepithelial lymphocytes. Int Immunol 1990;2:361–365. [PubMed: 1980616]
25. Reimann J, Rudolphi A. Co-expression of CD8αα in $CD4^+$ T cell receptor αβ T cells migrating into the murine small intestine epithelial layer. Eur J Immunol 1995;25:1580–1588. [PubMed: 7614985]
26. Wang HC, Dragoo J, Zhou Q, Klein JR. An intrinsic thyrotropin-mediated pathway of TNF-α production by bone marrow cells. Blood 2003;101:119–23. [PubMed: 12393601]
27. Morris AP, Estes MK. Microbes and microbial toxins: paradigms for microbial-mucosal interactions. VIII. Pathological consequences of rotavirus infection and its endotoxin. Am J Physiol Gastrointest Liver Physiol 2001;281:303–10.

28. Resigno M, Urbano M, Valzasina B, Francolini M, Rotta G, Bonasio R, Granucci F, Kraehenbuhl JP, Ricciardi-Castagnoli P. Dendritic cells express tight junction proteins and penetrate gut epithelial monolayers to sample bacteria. Nature Immunol 2001;2:361–67. [PubMed: 11276208]
29. Rescigno M, Rotta G, Valzasina B, Ricciardi-Castagnoli P. Dendritic cells shuttle microbes across gut epithelial monolayers. Immunobiology 2001;204:572–81. [PubMed: 11846220]
30. Wang HC, Zhou Q, Dragoo J, Klein JR. Most murine $CD8^+$ intestinal intraepithelial lymphocytes are partically but not fully activated T cells. J Immunol 2002;169:4717–22. [PubMed: 12391179]
31. Mazet F. The Fox and the thyroid: the amphioxus perspective. BioEssays 2002;24:696–99. [PubMed: 12210529]
32. Chuong CM, Chodankar R, Widelitz RB, Jiang TX. Evo-devo of feathers and scales: building complex epithelial appendages. Curr Opin Genet Dev 2002;10:449–56. [PubMed: 11023302]
33. Manley NR. Thymus organogenesis and molecular mechanisms of thymic epithelial cell differentiation. Semin Immunol 2000;12:421–28. [PubMed: 11085174]
34. Eales JG, McLeese JM, Holmes JA, Youson JH. Changes in intestinal and hepatic thyroid hormone during spontaneous metamorphosis of the sea lamprey, Petromyzon marinus. J Exp Zool 2000;286:305–12. [PubMed: 10653969]
35. MacDonald TT, Bajaj-Elliott M, Pender SL. T cells orchestrate mucosal shape and integrity. Immunol Today 1999;20:505–10. [PubMed: 10529778]
36. Ogasawara M. Overlapping expression of amphioxus homologs of the thyroid transcription factor-1 gene and thyroid peroxidase gene in the endostyle: insight into evolution of the thyroid gland. Dev Genes Evol 2000;210:231–42. [PubMed: 11180827]
37. Venkatesh TV, Holland ND, Holland LZ, Su MT, Bodmer R. Sequence and developmental expression of amphioxus AmphiNK2-1: insights into the evolutionary origin of the vertebrate thyroid gland and forebrain. Dev Genes Evol 1999;209:254–59. [PubMed: 10079369]
38. Ogasawara M, Shigetani Y, Suzuki S, Kuratani S, Satoh N. Expression of thyroid transcription factor-1 (TTF-1) gene in the ventral forebrain and endostyle of the aganathan vertebrate, Lampetra japonica. Genesis 2001;30:51–58. [PubMed: 11416863]
39. Mayer WE, Uinuk-Ool T, Tichy H, Gartland LA, Klein J, Cooper MD. Isolation and characterization of lymphocyte-like cells from a lamprey. Proc Natl Acad Sci (USA) 2002;99:14350–55. [PubMed: 12388781]
40. Uinuk-Ool T, Mayer WE, Sato A, Dongak R, Cooper MD, Klein J. Lamprey lymphocyte-like cells express homologs of genes involved in immunologically relevant activities of mammalian lymphocytes. Proc Natl Acad Sci (USA) 2002;99:14356–61. [PubMed: 12391333]
41. Abe E, Marians RC, Yu W, Wu XB, Ando T, Li Y, Iqbal J, Eldeiry L, Rajendren G, Blair HC, Davies TF, Zaidi M. TSH is a negative regulator of skeletal remodeling. Cell 2003;115:151–62. [PubMed: 14567913]
42. Shanahan F. Intestinal lymphoepithelial communication. Adv Exp Med Biol 1999;473:1–9. [PubMed: 10659340]

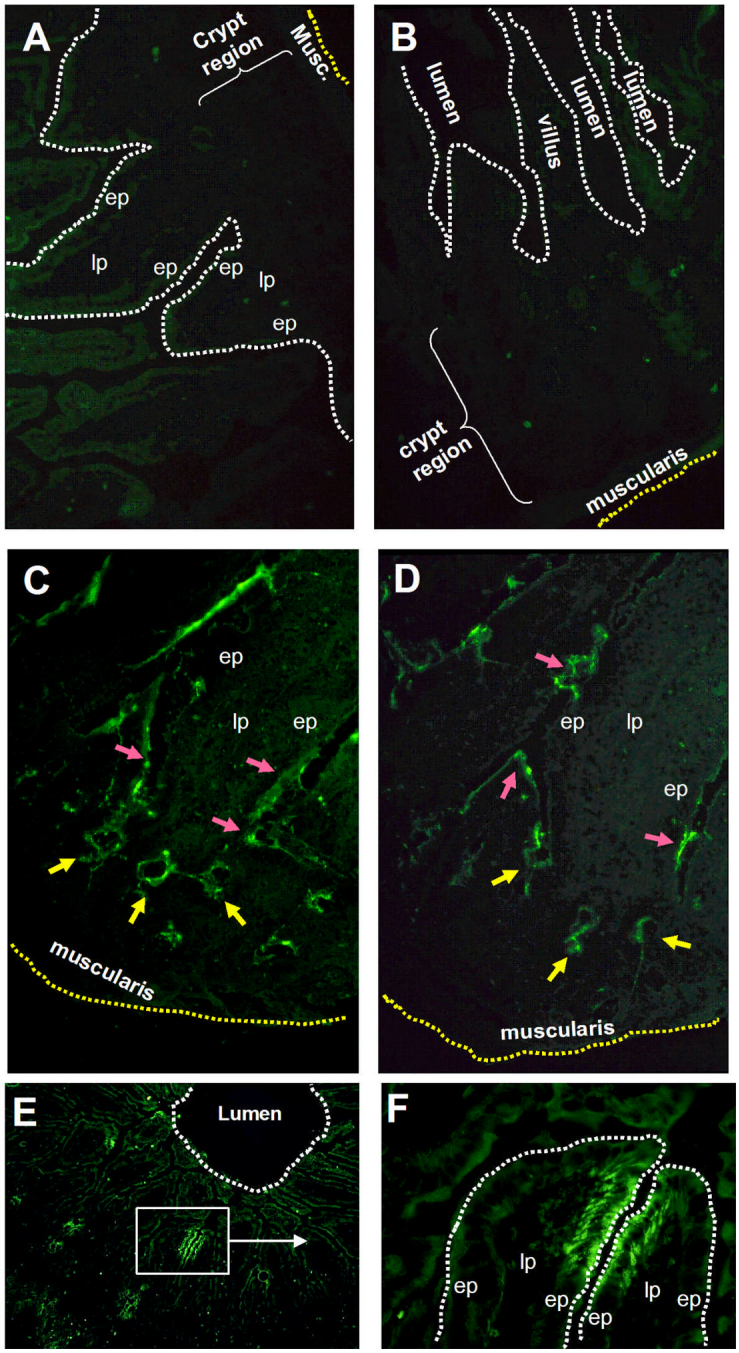

Fig. 1.

Panel A and B: jejunal sections from two different normal mice stained with biotinylated mouse Ig plus streptavidin-FITC. Panel C and D: TSH staining of jejunal sections showing localization of TSH in crypt regions (yellow arrows), as well as in the villus crypts and in areas just proximal to that (red arrows). Sections used in panels C and D are from the same animal as panel A. Panel E: TSH staining in upper regions of jejunal villi demonstrating the localized TSH hotblocks in apical lateral portion of some villi. Panel F: high-power magnification of boxed area from panel E showing the focal TSH staining pattern of two villi. Results are representative of six mice. Magnifications: A–C,F 400x; E 100x. (ep, epithelium; lp, lamina propria).

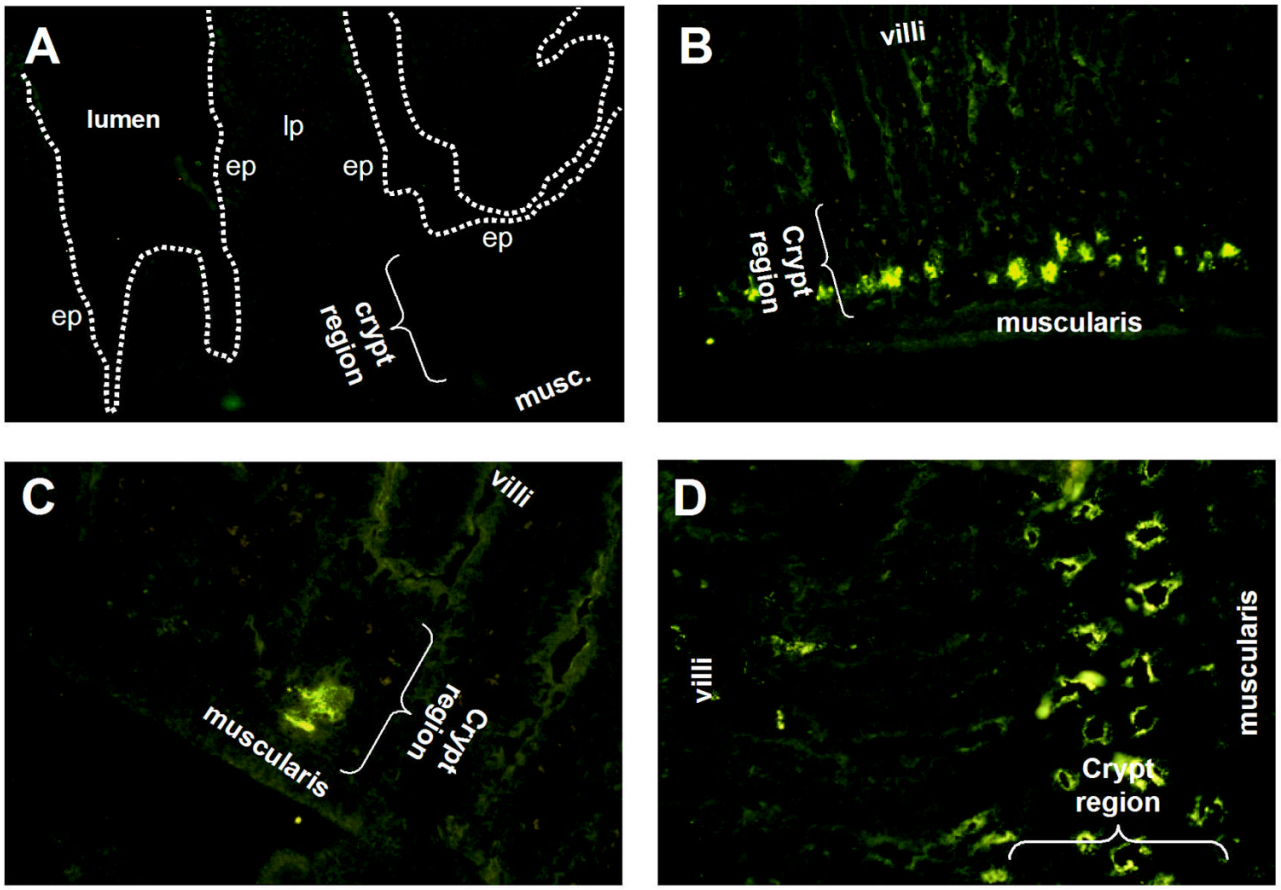

Fig. 2.

Panel A: jejunal section from a normal mouse stained with biotinylated mouse Ig plus streptavidin-FITC. Panel B and C: jejunal sections showing localization of TSH staining in the crypt regions; both sections are from the same animal. Panel D: jejunal section stained with anti-c-kit antibody demonstrating a concentration of c-kit in the crypt regions similar to where TSH staining occurs (see Fig. 1, panel C and D and Fig. 2 panel B and C for comparison). Results are representative of six mice, except for c-kit staining (panel D), which is representative of two mice. Magnifications: panel A and C 400x; panel B, 100x; panel D, 200x. (ep, epithelium; lp, lamina propria).

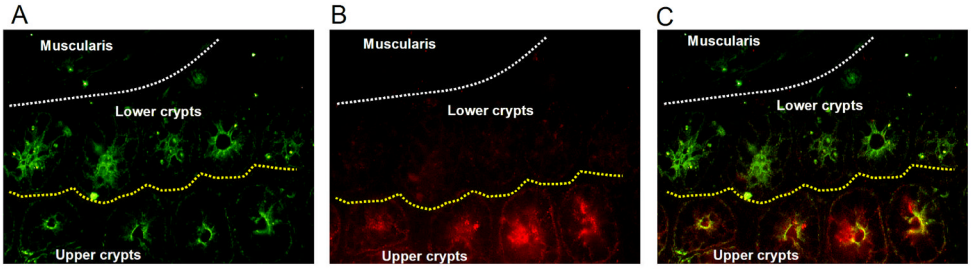

Fig. 3.

TSH staining in the mucosa is associated with areas of IL-7 staining. Panel A: under filtration that excluded red illumination of IL-7 staining, TSH staining was evident in both lower and upper crypt areas. Panel B: under filtration that excluded green illumination of TSH staining, IL-7 staining was localized only in upper crypt areas. Panel C: simultaneous examination of both regions confirmed those staining patterns, demonstrating clear evidence for simultaneous synthesis of TSH and IL-7 is some crypt areas, in particular those most distal to the muscularis. Results are representative of three mice. Magnification: Panel A–C, 400x.

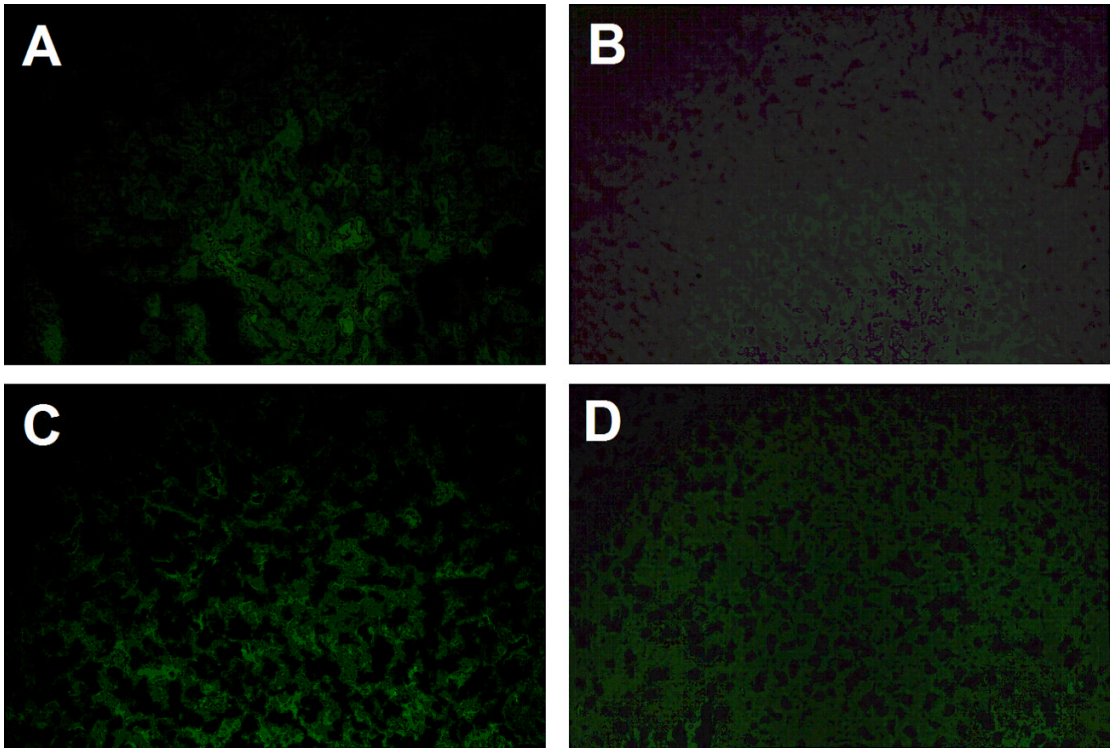

Fig. 4.

Panel A and B: control staining, and panel C and D: TSH staining of panel A and C: liver, and panel B and D: kidney tissue sections from the same animal used for jejunal sections in Fig. 1, panel A, C, and D. In general, TSH staining was minimal or absent compared to background staining. The low level of background staining may be due to binding of streptavidin-FITC to endogenous biotin in the liver and kidney. Results are representative of three mice. Magnifications: panel A–D, 200x.

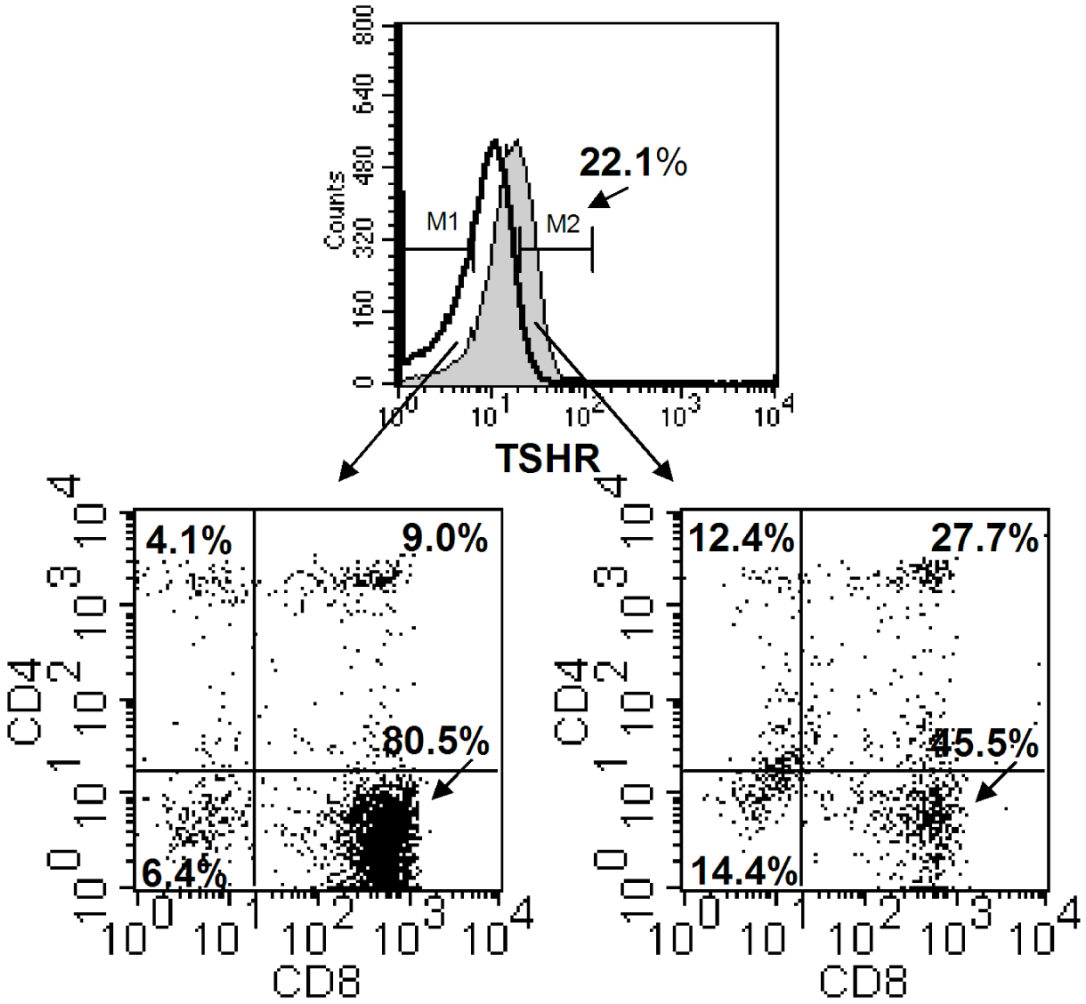

Fig. 5.

Three-color staining of small intestinal IELs for expression of TSHR, CD4, and CD8. Freshly-isolated IELs from normal mice were reacted with biotinylated bovine TSH and streptavidin-APC, plus PE-labeled anti-CD4 and FITC-labeled anti-CD8 mAbs as described in the Materials and methods. Control staining consisted of cells treated with streptavidin-APC, plus PE-labeled anti-CD4 and FITC-labeled anti-CD8 mAbs. In this experiment, the TSHR was expressed on 22.1% of the total IELs. The IELs consisted of four cell populations based on CD4 and CD8 expression, in proportions typical of IELs from normal mice [24]. Although the TSHR was expressed on all four cell populations, the majority of the $TSHR^+$ IELs were $CD8^+$ cells that included $CD4^-CD8^+$ and $CD4^+CD8^+$ cells. The remaining $TSHR^+$ cells were $CD4^+CD8^-$ cells or $CD8^-CD4^-$ cells. These findings demonstrate that some but not all IELs are TSH-responsive cells, and they indicate that TSH utilization is focused within specific groups of intestinal T cells. Results are representative of experiments from three mice.

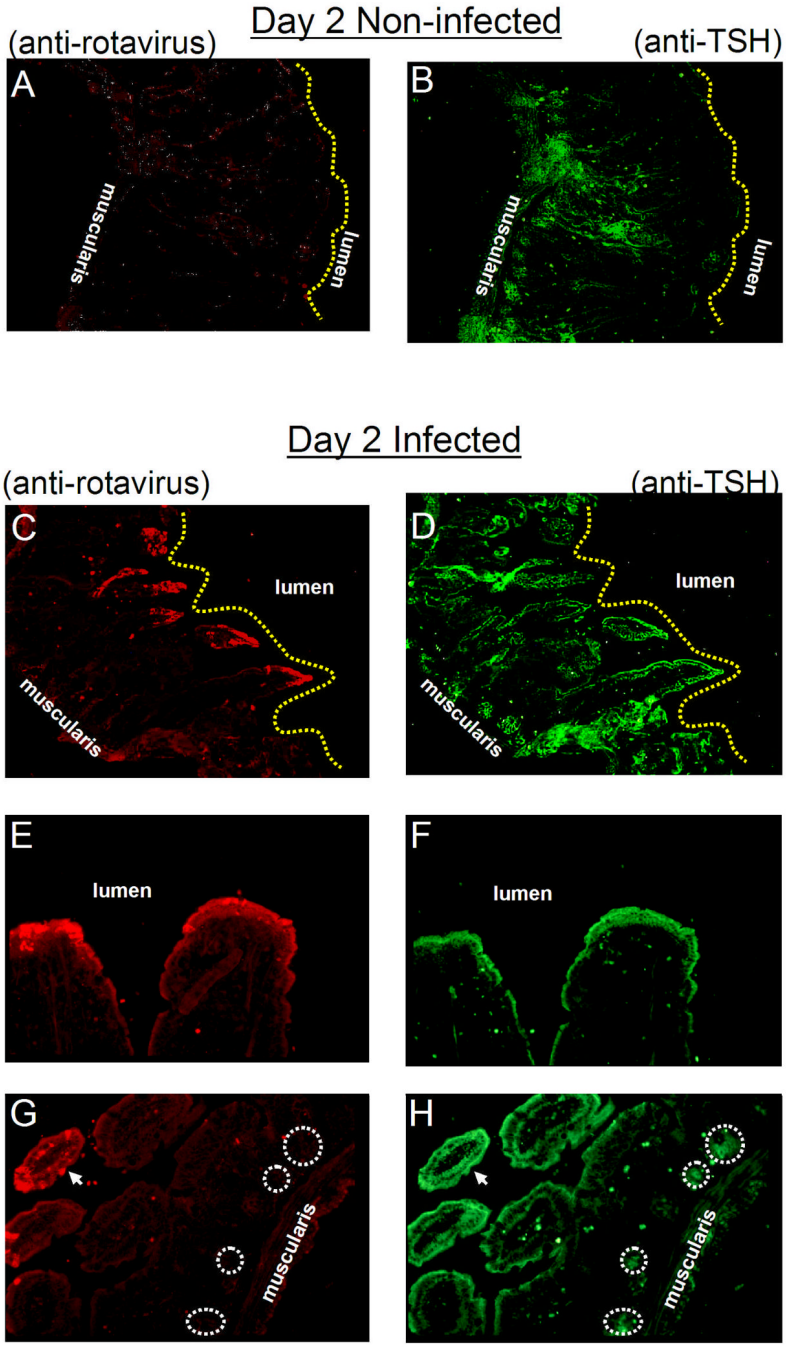

Fig. 6.

TSH expression in enterocytes of distal villi is upregulated during rotavirus infection. Panel A: intestinal tissues from non-infected mice do not stain with anti-rotavirus antibody, although as seen in panel B: they display a normal pattern of reactivity with anti-TSH antibody. Panel C: by day 2 post-rotavirus infection, the virus is localized in the apical region of the epithelium. Panel D: at that time, tissues display an increase in TSH staining in virus-infected areas. Panel E and F: rotavirus and TSH staining is localized in villus tips. Panel H: TSH synthesis continues in crypt regions where virus staining is absent, panel G. Results are representative of three mice. Magnifications: panel A–D, 100x; pane E and F, 400x; panel G and H, 200x. Circles

demarcate areas of TSH staining in the crypts (panel H) and the lack of virus staining in those areas (panel G).

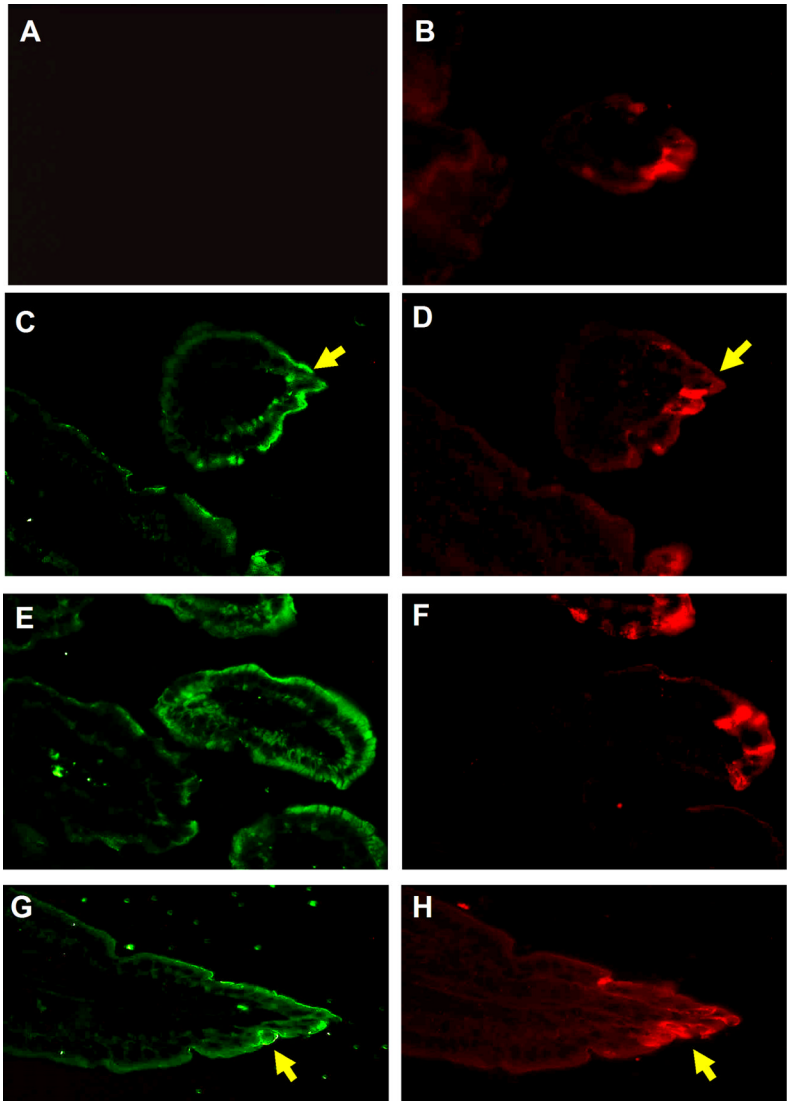

Fig. 7.

TSH and rotavirus staining of intestinal epithelia at 2 and 3 days post-infection. Staining of intestinal epithelia from mice 2 days post-infection (panel C and D) and 3 days post-infection (panel E–H) reveals TSH and rotavirus staining in villus tips the small jejunum. Panel A: staining of intestinal tissues with biotin-labeled control Ig plus streptavidin-FITC from (panel B) a rotavirus-infected mouse indicates that TSH staining of tissues was not due to non-specific antibody reactivity in infected regions. Results are representative of three infected mice. Magnifications: Panel A–H, 400x. Yellow arrows highlight some, though not all, of the regions where TSH staining and rotavirus staining are common.